Batteries & Supercaps

Research Article
doi.org/10.1002/batt.202400810

Chemistry Europe
European Chemical Societies Publishing

www.batteries-supercaps.org

Correlating Self-Discharge and Cycling Performance of Batteries to Fasten Electrolytes Development

Jiayi Zhang,[a] Boyu Wang,[a] and Laisuo Su*[a]

The development of next-generation batteries with high energy density requires the use of novel electrode materials with high specific energy density such as lithium metal anode, silicon anode, high-Ni $LiNi_xMn_yCo_zO_2$ cathode, and sulfur cathode. The stability of these materials and their poor compatibility with conventional electrolytes limit their application, and developing novel electrolytes is one of the most promising strategies to tackle the challenge. The current electrolyte development highly relies on expert knowledge and expertise through a trial-and-error approach, which is very time-consuming. Machine learning (ML) and artificial intelligence (AI) approaches have attracted attention to accelerating the process. However, gathering high-quality data from experimental procedures to train ML models is a laborious process, especially when the problem statements cross over to device-level applications. Here, we find a strong correlation between the self-discharge behavior of lithium-metal batteries and their cycling aging performance. As the self-discharge measurement can be done within a few days compared to months for cycling tests, the finding provides a strategy to collect high-quality data in a short period that can be used as input for ML and AI approaches for developing advanced electrolytes in next-generation batteries.

Introduction

Lithium-ion batteries (LIBs) have achieved great success in electrifying our society. However, the limited energy density (300 $W\,h\,kg^{-1}$) of LIBs with graphite as the anode can hardly meet the demand for the driving range of electric vehicles (500 km).[1] There is an urgent need to develop next-generation battery technology with high energy density. Although many battery materials with high energy densities have been discovered, such as Li and Si anode, their application in practical batteries is hindered by poor compatibility with state-of-the-art electrolytes. The discovery and optimization of battery electrolytes have become the bottleneck for developing high-energy-density batteries. The battery electrolyte typically has one or more organic solvents and one or more salts/additives. The choice of solvents, salts, additives, and their molar ratio has been shown to have significant impacts on many battery performance outcomes such as capacity retention, rate performance, and safety.[2–5] Currently, electrolyte development still highly relies on expert knowledge and expertise through a trial-and-error approach. This approach is effective but very time-consuming, resulting in a slow electrolyte development process in the past three decades.

The rapid development of ML algorithms has stimulated their applications in the battery field in the past decade,[6] including battery design,[7] test protocol optimization,[8] cycle life prediction,[9] and novel materials discovery.[10] The application of ML and AI has recently attracted attention for developing liquid electrolytes in LIBs,[11] such as unveiling electrolyte chemistry principles based on a data-driven approach[12] and developing knowledge-data dual-driven machine learning framework to predict electrolyte properties.[13] However, the constraint of producing sufficient high-quality data limits the application of ML for developing battery electrolytes. For example, a recent study by Kim et al. in 2023 contained 150 data points collected from the literature.[14] Although the study is an excellent example of a data-driven electrolyte design strategy, the method may not be generalizable as all the features are extracted by human experts who skim over crucial structural and compositional information. Moreover, the data collected from various literature is from batteries tested with different conditions by different experimenters that contain uncontrollable bias. Therefore, gathering high-quality data from experimental procedures to train ML models is a laborious process, especially when the problem statements cross over to device-level applications, such as in the case of battery electrolyte development.

A general electrolyte development procedure for LIBs or any other types of battery includes four general steps (Figure 1), which are (1) proposing electrolyte composition, (2) fabricating batteries, (3) testing batteries, and (4) analyzing data. Among these four steps, the battery testing step is usually the most time-consuming because battery aging performance needs to be tested under cycling and/or storage.[9,15] The cycling tests are the most used, where batteries are cycled at a fixed rate for charge and discharge or used a modification of different expected use profiles, which takes months and even years to complete.[16] The storage tests include a combination of extended hold periods and intermitted data acquisition to capture information on capacity fade and impedance change, which takes even longer compared to cycling tests.[17] Therefore,

[a] J. Zhang, B. Wang, L. Su
Department of Materials Science and Engineering, University of Texas at Dallas, Richardson, TX-75080, USA
E-mail: laisuo.su@utdallas.edu

Supporting information for this article is available on the WWW under https://doi.org/10.1002/batt.202400810

Research Article
doi.org/10.1002/batt.202400810
Chemistry Europe
European Chemical Societies Publishing

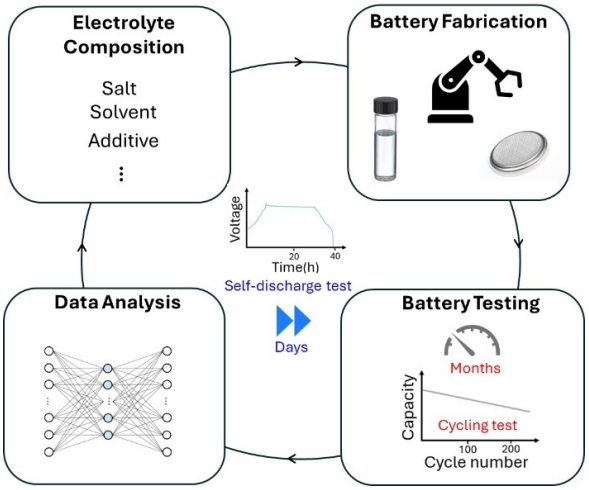

Figure 1. A schematic shows the research development process for electrolyte composition optimization that generally has four steps, including proposing electrolyte composition, battery fabrication, battery testing, and data analysis. The battery testing is the limiting step when applying a normal cycling test, and thus, replacing the cycling test with a self-discharge test can largely accelerate the electrolyte development process.

developing an alternative testing method that can represent the long-term cycling performance of a battery is crucial to gathering high-quality data because it is a prerequisite before scientists can leverage data-driven methods for formulation space.

The self-discharge behavior of batteries has been studied in many research papers, and the test can be done within a few days or even a few hours at high temperatures. We noticed in our previous study that $LiNi_xMn_yCo_zO_2$ (NMC) cathode-based LIBs with slow self-discharge rates show better cycling performance.[5] A recent study also found that Na-Ion batteries with $NaNi_{1/3}Fe_{1/3}Mn_{1/3}O_2$ cathode exhibit a self-discharge behavior similar to that of high-Ni NMC811 LIBs.[18] If the self-discharge behavior of a battery can be correlated to its cycling performance, the test time of electrolyte-electrode compatibility can be significantly reduced to generate sufficient high-quality data for ML/AI models.

In this study, we collected literature data to analyze the relationship between the self-discharge behavior of NMC-based LIBs and their cycling performance. We found that self-discharge of LIBs is a good indicator of the compatibility between the NMC-based cathodes and electrolytes. The strong correlation between self-discharge and cycling performance is also validated in our experiments using three different types of NMC cathodes. It is worthwhile extending our analysis to other types of electrode materials, including both cathodes and anodes and other battery systems when sufficient relevant data becomes available in literature.

Results and Discussion

Literature Data on Cycling Aging and Self-Discharge of LIBs

To uncover the relationship between the capacity fading during the cycling test or calendar test and the self-discharge behavior of LIBs, we first summarize the existing data in the literature. It is worth noting that the majority of battery-relevant papers present either cycling performance, calendar aging performance, or self-discharge behavior. Very few papers reported all these performances in one study. Moreover, the self-discharge studies in the limited papers were conducted at different temperatures and different periods, and the cycling tests were conducted at different C-rates. It is very hard to find high-quality data to correlate capacity fading and self-discharge of LIBs.

Figure 2a summarizes all the relevant data points we found in the literature that studies NMC cathode-based LIBs. Almost all of them are from the same research group (Prof. Manthiram at UT Austin), which helps reduce human error to some degree. The battery compositions and testing conditions are summarized in Table S1 in Supporting Information. The raw data in Figure 2a suggests that there is no clear relationship between capacity retention during cycling and self-discharge retention. However, the tests in different studies were conducted under different conditions. To be more specific, Figure 2b shows the self-discharge tests were conducted at different temperatures with different storage times, both of which affect the self-discharge capacity retention of LIBs. Similarly, Figure 2c shows the cycling tests in the literature were conducted at different C-rates with different cycle numbers. Thus, it is crucial to normalize the self-discharge capacity retention and cycling capacity retention in different studies by considering these factors.

To normalize the self-discharge capacity loss, we considered both the self-discharge storage time and temperature. We assume that all the self-discharges were tested within the temperature range that does not change the side reaction mechanisms, and thus the impact of temperature on the self-discharge rate (k_s) can be described by Arrhenius's law: $k_s(T) = A \cdot exp\left(-\frac{Q}{RT}\right)$. Where A, Q, and R are constant, T is temperature. A factor "$\exp\left(\frac{1}{T}\right)$" is used to control the impact of temperature on the k_s. We used "$exp\left(\frac{1}{T-25}\right)$" in the k_s to normalize the side reaction rate to room temperature at 25 °C. The open circuit voltage (OCV) of a battery does not change much during the self-discharge process in most of the tests reported in the literature, and thus, the self-discharge capacity retention (SCR) decreases linearly with the time of the self-discharge test. As a result, a factor "$\frac{(1-SCR)}{t}$" can be considered as the average storage capacity loss ($1 - SCR$) per hour. We normalized the storage time to 100 hours to calculate the k_s. Therefore, the normalized self-discharge rate (k_s) can be expressed in the following formula.

Research Article
doi.org/10.1002/batt.202400810
Chemistry Europe
European Chemical Societies Publishing

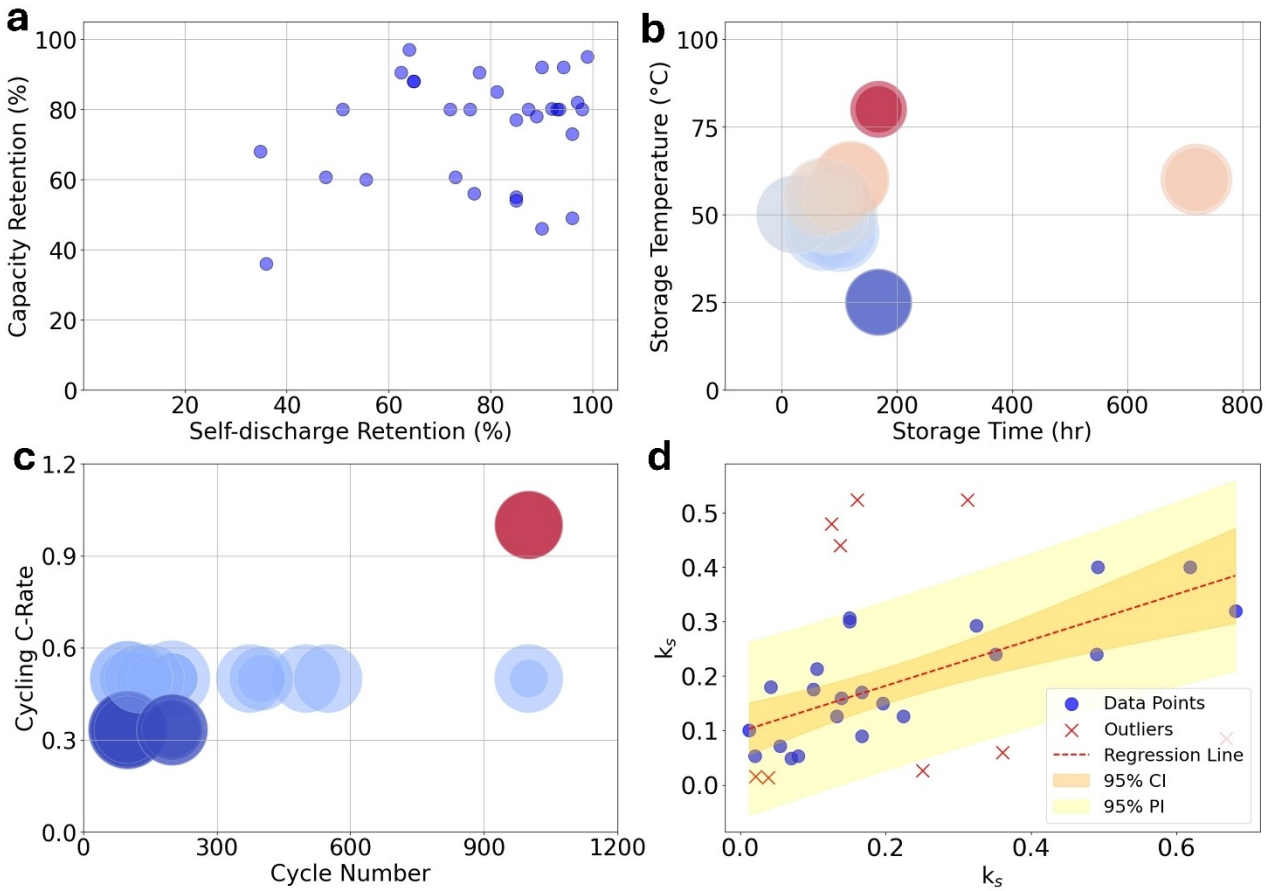

Figure 2. A summary of literature data on NMC-based LIBs. (a) The figures of self-discharge retention and cycling capacity retention of LIBs quoted directly from the literature. (b) The schematic illustrating the relationship between storage time, storage temperature, and storage capacity retention reported in the literature. The size of the circle represents the storage capacity retention of different data points. (c) The schematic illustrating the cycle capacity retention reported with different C-rate and at different cycle numbers. The size of the circle represents the cycling capacity retention of different data points. (d) The linear relationship between normalized self-discharge and normalized cycling performance after ruling out outliers. The orange and yellow intervals represent the 95% confident interval and 95% prediction interval, respectively.

$$k_s(100\ h,\ 25\ ^\circ C) = \frac{100(1-SCR)}{t} exp\left(\frac{1}{T-25}\right)$$

Where SCR is the storage capacity retention reported in the literature, t is the storage time in the unit of h, and T is the storage temperature in the unit of °C and T > 25 °C.

To normalize the cycling capacity loss, we considered both the number of cycles and the cycling C-rate during the test. We noticed that the capacity fading is almost proportional to the cycle number in most NMC-based LIBs.[4,5,19] Moreover, the capacity fading of LIBs during cycling is found to be proportional to the cycling C-rate in some studies.[20,21] Thus, the capacity fading is normalized to the test at C/3 for 200 cycles using the following formula.

$$k_c(200\ cycle,\ C/3) = \frac{200(1-CCR)}{n} \times \frac{C/3}{C\_rate}$$

Where CCR is the cycling capacity retention reported in the literature, n is the number of cycles, and C-rate is the cycling C-rate.

Figure 2d shows the normalized self-discharge (k_s) and normalized cycling performance (k_c) of NMC-based LIBs in the literature. A few outliers are identified from the results, and the methodology of identifying outliers will be discussed in the later section of this paper. The results suggest a strong correlation between the normalized self-discharge and normalized cycling performance. It needs to be noted that inconsistency and human errors are unavoidably introduced during these studies over five years conducted by different students, such as the glovebox environments, different electrolyte amounts used, room temperature fluctuation, etc. The strong correlation between k_c and k_s suggests that an NMC-based LIB with faster self-discharge will also have a faster cycling capacity fading, regardless of the electrolytes and electrodes used in the battery. Therefore, the self-discharge test can be used as an alternative testing method to evaluate the performance of an electrolyte in NMC-based LIBs.

Research Article
doi.org/10.1002/batt.202400810
Chemistry Europe
European Chemical Societies Publishing

Correlation Analysis of Testing Parameters and Battery Performance

Pearson and Spearman correlation coefficients are benchmarks for measuring the relationship between two variables.[22] Specifically, the Pearson correlation coefficient quantifies the strength and direction of a linear relationship between two variables, assuming normality and linearity, with values ranging from -1 to $+1$. In contrast, Spearman correlation is a non-parametric method that assesses the monotonic relationship between variables, requiring no specific distribution assumptions and making it suitable for ranked or ordinal data.[23,24] We applied both methods to correlate all the experimental parameters, cycling capacity fading, and self-discharge behavior to examine our previous analysis and conclusion. All the raw data summarized from the literature is summarized in Table S1.

Figure 3 shows that cycling capacity retention ("Cycle Retention") is negatively related to the cycle number and cycling C-rate ("C-rate"), which agrees with that in the literature.[25] The Pearson correlation coefficients of cycle capacity retention on the cycle number and cycling C rate are -0.3 and -0.2, while the Spearman correlation coefficients of cycle capacity retention on the cycle number and cycling C rate are -0.6 and -0.3. The lower absolute coefficient values in Person analysis are derived from its linear constraint. The negative sign indicates that the cycling capacity retention decreases with the increase of cycle number and C-rate, which agrees with our analysis of the normalized cycling performance (k_c). Similarly, the correlation coefficients of self-discharge capacity retention ("Self-dischar Retention") on temperature and time are both negative. The negative sign also indicates that self-discharge retention decreases with the increase in temperature and time which agrees with our analysis of the normalized self-discharge (k_s). The Pearson and Spearman correlation coefficients of normalized k_s and $k_c$are 0.8 and 0.7, demonstrating a strong positive correlation between them.

Outliers Identification via Statistical Analysis

The experimental data was collected over five years by different students at different lab locations. Moreover, the battery format, anode materials, and electrolyte amount are not consistent in all the experiments, which could lead to outliers among these data. To identify outliers from experimental errors, the random sampling method was applied to analyze the influence of sample size on the correlation coefficient among k_s and k_c. Figure 4a shows that the Spearman coefficient decreases with the increase of the sample size, and a rapid decrease appears when the sample size goes beyond 24, indicating that there are around seven outliers among the 31 data points. However, random sampling was used for Spearman analysis and different number of combinations were applied to reduce the computational cost, which could lead to poor accuracy. More accurate statistical methods were further applied to identify outliers.

DBSCAN and K-Means algorithms are used to identify outliers in this study. DBSCAN is a density-based clustering algorithm that groups points based on their density without requiring the number of clusters.[26] It identifies core points that have a minimum number of neighboring points within a specified radius (*eps*) and expands clusters from these core points. Data points exhibiting significant discrepancies or errors tend to deviate from the main distribution. By analyzing dense and sparse regions, we can identify outliers from the dataset without relying on predefined cluster shapes. As it has been reported that the degradation mechanisms of LIBs depend on cycling C-rates, we identified the outliers at different C-rates individually (Figure 4b, c). The parameters $eps_1 = 0.17$ and

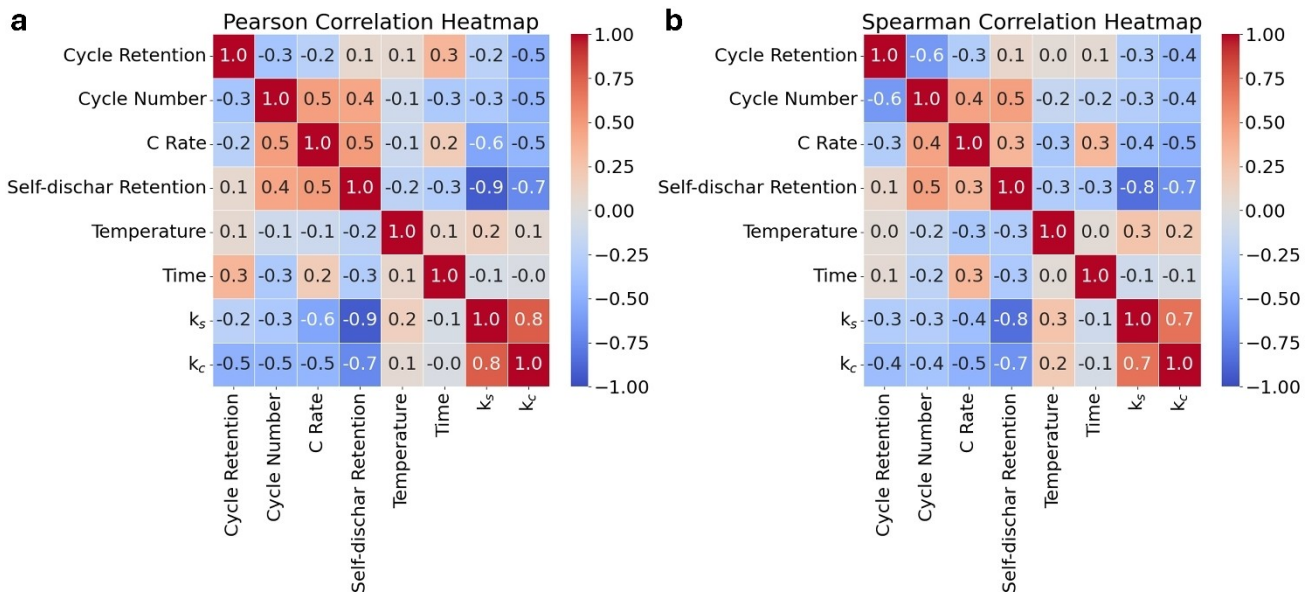

Figure 3. The correlation analysis of different features in the self-discharge test and cycling test with (a) Pearson correlation analysis and (b) Spearman correlation analysis.

Research Article
doi.org/10.1002/batt.202400810
Chemistry Europe
European Chemical Societies Publishing

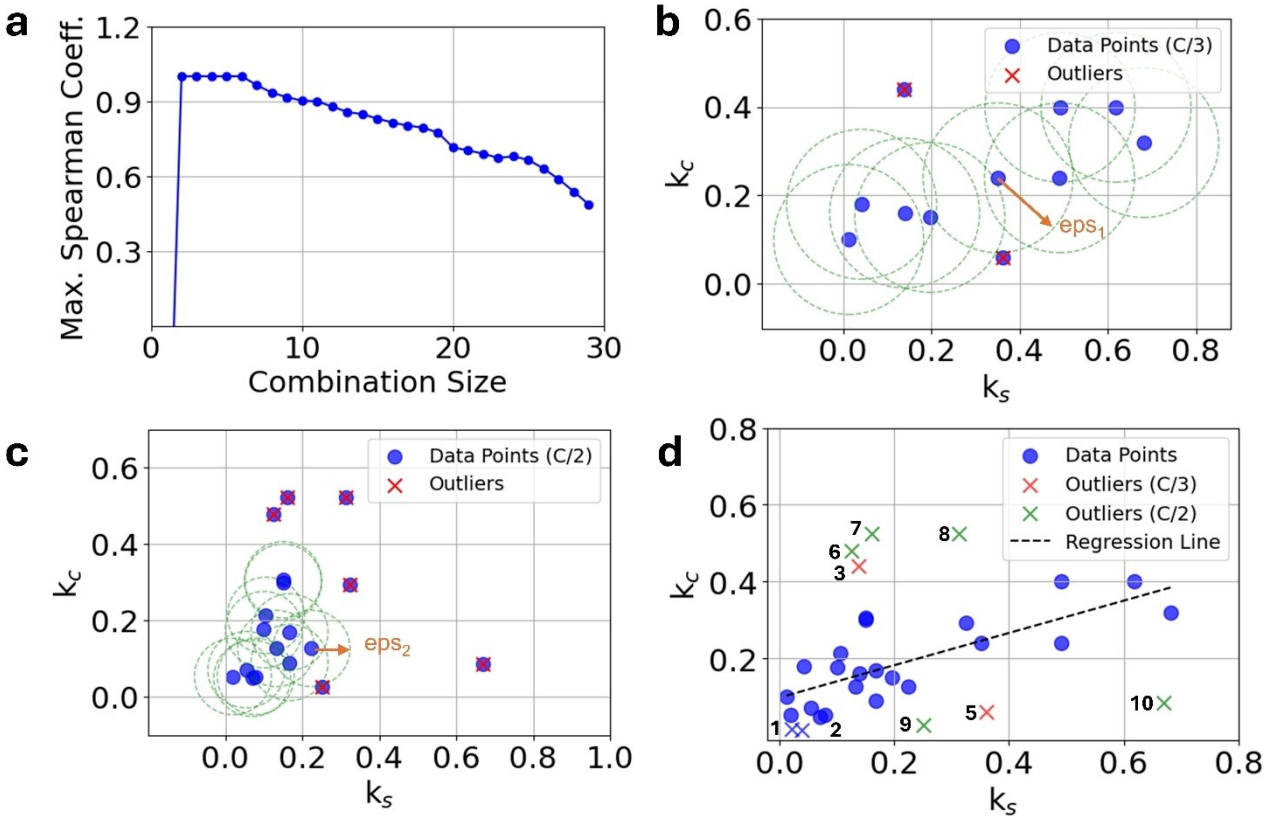

Figure 4. Summary of outlier identification and features analysis of outliers. (b, c) Principle and results of DBSCAN clustering analysis for (b) C/3 rate and (c) C/2 rate. (d) The linear regression of normalized self-discharge and normalized cycling performance with outliers labeled.

$eps_2 = 0.1$ were determined based on the distribution of data points. Points that do not meet the density requirement for inclusion in a cluster are identified as outliers because they lack sufficient neighboring points within the specified *eps* radius.

K-means clustering is also used to identify outliers from the datasets by grouping data points into clusters based on proximity to centroids (Figure S1). However, K-Means has inherent limitations as it forces each data point into a cluster and thus cannot explicitly classify data points as noise or outliers. The centroids are affected by outliers, resulting in unreliable clustering when outliers are present. In other words, K-Means cannot differentiate between core data points and genuine outliers, leading to potentially misleading clustering results. Thus, the DBSCAN algorithm was used to identify outliers by classifying low-density points.

Figure 4b, c shows that the DBSCAN algorithm identifies two outliers from cycling data tested at C/3 and six outliers from cycling data tested at C/2. However, one of these outliers (data point 4 in Figure S2) aligns well with the general trend of normal data points and thus should be included in the analysis. This mislabeling of data points indicates the limitation of applying the DBSCAN algorithm for outlier identification, and the determination of outliers is related to the choice of algorithms and parameters such as the *eps* value of the DBSCAN algorithm. The seven outliers are labeled in Figure 4d (data points 3, 5–10). To understand the causes of these outliers, we analyzed the cycling performance and self-discharge testing of these papers. The cycling behavior of LIBs that correspond to the data points 3, 5, 7, and 8 are not linear,[27–29] and thus the linear treatment to normalize the cycling capacity retention (k_c) of these data points can cause unexpected errors. The study corresponding to the data point 6 was done in batteries with two different anode materials, where the cycling test was tested in LIBs with SiO_x/Graphite anode while the self-discharge test was conducted in LIBs with Li metal anode.[30] Thus, the relationship between $k_c$and k_s of data point 6 is deviated from those tested in the same battery. For data points 9 and 10, the cycling test was conducted in pouch cells, while the self-discharge test was conducted in coin cells.[31] Besides the seven identified outliers, we also excluded data points 1 and 2 for the correlation analysis. The cycling test of the LIBs corresponding to these two data points was conducted at 1 C,[32] the only two data points at the C-rate. After excluding the nine data points (seven outliers and two data points tested at 1 C), the remaining data points in Figure 4d show a strong correlation between the k_s and k_c.

Validating the k_s and k_c Relationship

To validate the relationship between k_s and k_c as shown in Figure 4d, three types of LIBs are made using Li metal as the anode and LP57 as the electrolyte (1 M $LiPF_6$ in EC/EMC 3/7 by weight). The cathode materials in the three types of LIBs are

Research Article
doi.org/10.1002/batt.202400810
Chemistry Europe
European Chemical Societies Publishing

different NMC811 materials, including a fresh single crystal NMC811, a fresh polycrystal NMC811 (polycrystal 1), and an aged polycrystal NMC811 (polycrystal 2) stored in a glove box for one year. All the other conditions were kept the same during battery fabrication.

The three types of LIBs were tested under cycling at a C/2C-rate. Figure 5a shows that the cycling capacity retention for single crystal NMC811, NMC811 (polycrystal 1), and NMC811 (polycrystal 2) are 90.9%, 72.4%, and 64.5% after 200 cycles, respectively. Moreover, a self-discharge test was conducted at the fully charged status at 50 °C for all the LIBs. Figure 5b shows that the self-discharge capacity retention for single crystal NMC811, NMC811 (polycrystal 1), and NMC811 (polycrystal 2) are 97.8%, 97.3%, and 95.2% after 20 hours, respectively. A self-discharge for 100 hours was also conducted, and the result is shown in Figure S3. Compared to the cycling test that took over one month to complete, the self-discharge experiment took less than two days, a significant acceleration of the experiment procedure.

Figure 5c displays our experimental data together with literature data. Two coin cells were tested in the same conditions, and thus there are a total of 12 data points (6 data points at storage test for 20 hours, and 6 data points for 100 hours). The normalized cycling performance (k_c) of single crystal NMC811, NMC811 (polycrystal 1), and NMC811 (polycrystal 2) are 0.0606, 0.184, and 0.236, respectively. The normalized self-discharge (k_s) of single crystal NMC811, NMC811 (polycrystal 1), and NMC811 (polycrystal 2) are 0.100, 0.106, and 0.231, respectively, for 20 hours storage test, and are 0.0508, 0.0546, and 0.130, respectively, for 100 hours storage test. All the data tested lies within the 95% prediction interval obtained from literature data, validating the strong correlation between self-discharge performance and cycling capacity fading behavior.

Conclusions

Testing the longevity of batteries to examine the compatibility of electrolytes against electrode materials is a time-consuming process, limiting the applicability of the ML/AI method to accelerate the development of advanced electrolytes for next-generation batteries. Here, we demonstrate using self-discharge testing to examine the performance of electrolytes for NMC-based cathodes, which can largely shorten the test time from months of conventional cycling tests to a few days. The rationality of applying self-discharge testing is from a strong correlation between cycling capacity retention and self-discharge retention by analyzing literature data. Such a correlation is also proved by our laboratory data using different types of

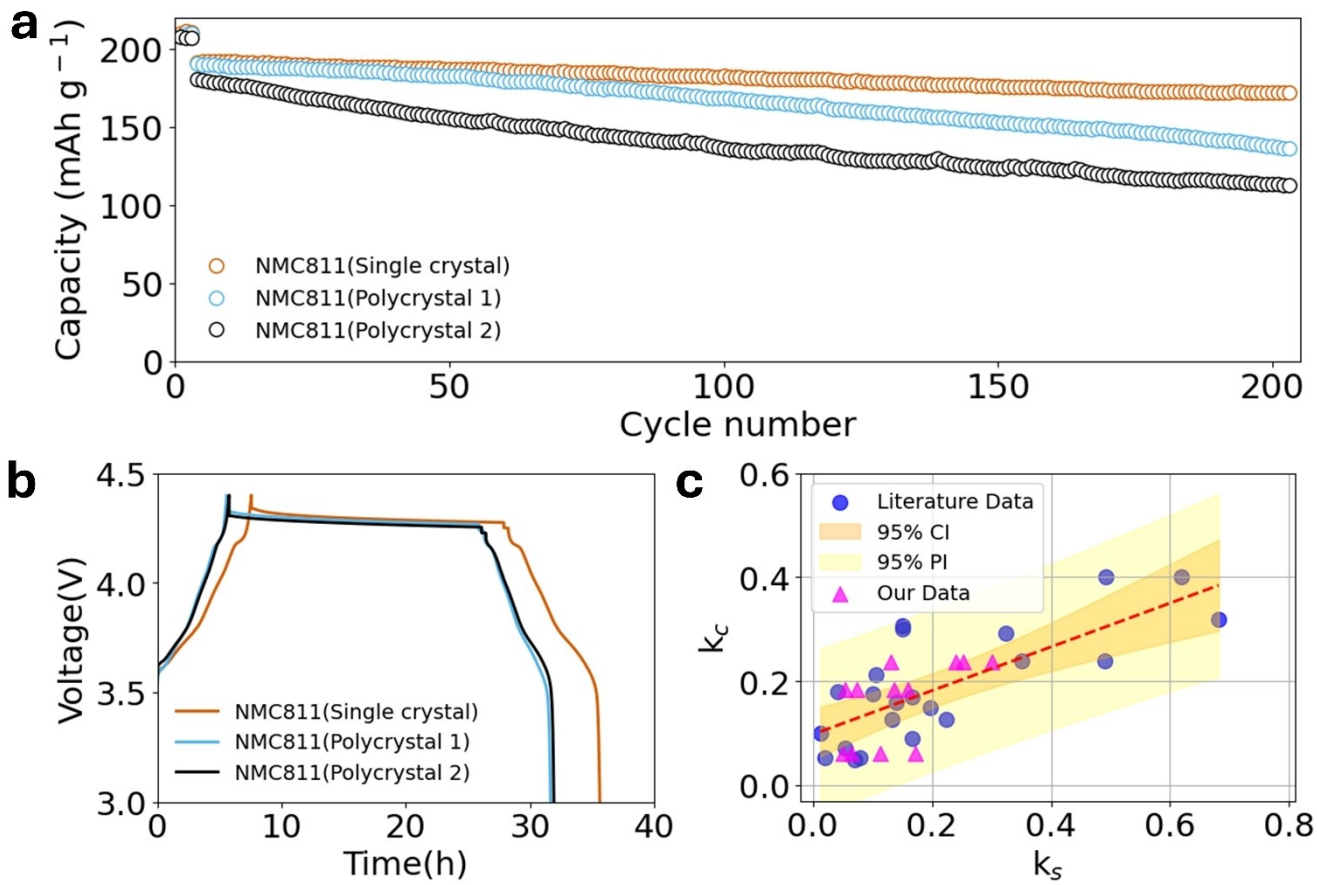

Figure 5. Experimental validation of the relationship between cycling test performance and self-discharge behavior. (a) The capacity fading of three types of NMC811 cathodes cycled at C/2 C-rate. (b) Self-discharge test of the three NMC811 cathodes for 20 hours. (c) The correlations between normalized cycling performance (k_c) and the normalized self-discharge (k_s) of the tested samples.

NMC811 cathode materials. Although our study is limited to LIBs with NMC cathode, the methodology can be extended to other cathode materials and other battery systems such as lithium-sulfur batteries and sodium-sulfur batteries. Applying self-discharge testing could also significantly shorten the evaluation times for these batteries and thus warrant further evaluation.

We found challenges when collecting high-quality data to correlate the self-discharge performance and cycling performance of batteries. As collecting high-quality data is a major prerequisite before data-driven methods can be applied to guide experiment design and draw meaningful conclusions, we strongly recommend the battery community standardize testing protocols for battery development in future studies. Moreover, all the data was manually extracted by human experts. The process is time-consuming and may miss some useful data in the literature. AI-based information extraction methods should be considered and developed that can obtain desired information from published data in future studies.

Acknowledgements

The authors acknowledge the New Faculty startup funding provided by the University of Texas at Dallas. This project was also funded by The University of Texas at Dallas Office of Research and Innovation through the New Faculty Research Symposium Grant Program.

Conflict of Interests

The authors declare no conflict of interest.

Data Availability Statement

The data that support the findings of this study are available in the supplementary material of this article.

Keywords: Battery · Electrolytes · Self-discharge · Cycling performance · Machine learning

[1] L. Su, A. Manthiram, *Small Struct.* **2022**, *3*, DOI: 10.1002/sstr.202200114.
[2] J. He, A. Bhargav, L. Su, J. Lamb, J. Okasinski, W. Shin, A. Manthiram, *Nat. Energy* **2024**, *9*, 446.
[3] L. Su, X. Zhao, M. Yi, H. Charalambous, H. Celio, Y. Liu, A. Manthiram, *Adv. Energy Mater.* **2022**, *12*, DOI: 10.1002/aenm.202201911.
[4] M. Yi, L. Su, A. Manthiram, *J. Mater. Chem. A* **2023**, *11*, 11889.
[5] L. Su, E. Jo, A. Manthiram, *ACS Energy Lett.* **2022**, *7*, 2165.
[6] X. Chen, X. Liu, X. Shen, Q. Zhang, *Angew. Chem. Int. Ed.* **2021**, *60*, 24354.
[7] K. T. Schütt, F. Arbabzadah, S. Chmiela, K. R. Müller, A. Tkatchenko, *Nat. Commun.* **2017**, *8*, 13890.
[8] P. M. Attia, A. Grover, N. Jin, K. A. Severson, T. M. Markov, Y.-H. Liao, M. H. Chen, B. Cheong, N. Perkins, Z. Yang, P. K. Herring, M. Aykol, S. J. Harris, R. D. Braatz, S. Ermon, W. C. Chueh, *Nature* **2020**, *578*, 397.
[9] L. Su, M. Wu, Z. Li, J. Zhang, *eTransportation* **2021**, *10*, 100137.
[10] N. J. Szymanski, B. Rendy, Y. Fei, R. E. Kumar, T. He, D. Milsted, M. J. McDermott, M. Gallant, E. D. Cubuk, A. Merchant, H. Kim, A. Jain, C. J. Bartel, K. Persson, Y. Zeng, G. Ceder, *Nature* **2023**, 1.
[11] A. Dave, J. Mitchell, S. Burke, H. Lin, J. Whitacre, V. Viswanathan, *Nat. Commun.* **2022**, *13*, 5454.
[12] Y.-C. Gao, N. Yao, X. Chen, L. Yu, R. Zhang, Q. Zhang, *J. Am. Chem. Soc.* **2023**, *145*, 23764.
[13] Y. Gao, Y. Yuan, S. Huang, N. Yao, L. Yu, Y. Chen, Q. Zhang, X. Chen, *Angew. Chem. Int. Ed.* **2025**, *64*, e202416506.
[14] S. C. Kim, S. T. Oyakhire, C. Athanitis, J. Wang, Z. Zhang, W. Zhang, D. T. Boyle, M. S. Kim, Z. Yu, X. Gao, T. Sogade, E. Wu, J. Qin, Z. Bao, S. F. Bent, Y. Cui, *Proc. Natl. Acad. Sci.* **2023**, *120*, e2214357120.
[15] L. Su, J. Zhang, C. Wang, Y. Zhang, Z. Li, Y. Song, T. Jin, Z. Ma, *Appl. Energy* **2016**, *163*, 201.
[16] E. J. Dufek, T. R. Tanim, B.-R. Chen, S. Kim, *Joule* **2022**, *6*, 1363.
[17] L. Su, J. Zhang, J. Huang, H. Ge, Z. Li, F. Xie, B. Y. Liaw, *J. Power Sources* **2016**, *315*, 35.
[18] L. Streck, T. Roth, H. Bosch, C. Kirst, M. Rehm, P. Keil, A. Jossen, *J. Electrochem. Soc.* **2024**, *171*, 080531.
[19] R. Sim, L. Su, A. Manthiram, *Adv. Energy Mater.* **2023**, *13*, DOI: 10.1002/aenm.202300096.
[20] S. Saxena, Y. Xing, D. Kwon, M. Pecht, *Int. J. Electr. Power Energy Syst.* **2019**, *107*, 438.
[21] R. Gauthier, A. Luscombe, T. Bond, M. Bauer, M. Johnson, J. Harlow, A. J. Louli, J. R. Dahn, *J. Electrochem. Soc.* **2022**, *169*, DOI: 10.1149/1945-7111/ac4b82.
[22] E. van den Heuvel, Z. Zhan, *Am. Stat.* **2022**, *76*, 44.
[23] A. G. Dufera, T. Liu, J. Xu, *Stat. Theory Relat. Fields* **2023**, *7*, 97.
[24] H. Yu, A. D. Hutson, *Commun. Stat. - Theory Methods* **2024**, *53*, 2141.
[25] T. R. Tanim, Z. Yang, D. P. Finegan, P. R. Chinnam, Y. Lin, P. J. Weddle, I. Bloom, A. M. Colclasure, E. J. Dufek, J. Wen, Y. Tsai, M. C. Evans, K. Smith, J. M. Allen, C. C. Dickerson, A. H. Quinn, A. R. Dunlop, S. E. Trask, A. N. Jansen, *Adv. Energy Mater.* **2022**, *12*, DOI: 10.1002/aenm.202103712.
[26] D. Deng, *2020 7th Int. Forum Electr. Eng. Autom. (IFEEA)* **2020**, *00*, 949.
[27] C. Liu, Z. Cui, A. Manthiram, *Adv. Energy Mater.* **2024**, *14*, DOI: 10.1002/aenm.202302722.
[28] S. Lee, G. Song, B. Yun, T. Kim, S. H. Choi, H. Kim, S. W. Doo, K. T. Lee, *ACS Nano* **2024**, *18*, 10566.
[29] M. Yi, W. Li, A. Manthiram, *Chem. Mater.* **2022**, *34*, 629.
[30] M. Yi, Z. Cui, A. Manthiram, *ACS Appl. Mater. Interfaces* **2024**, *16*, 42270.
[31] Q. Xie, A. Manthiram, *Chem. Mater.* **2020**, *32*, 7413.
[32] W. Li, A. Dolocan, J. Li, Q. Xie, A. Manthiram, *Adv. Energy Mater.* **2019**, *9*, DOI: 10.1002/aenm.201901152.
[33] R. Pan, E. Jo, Z. Cui, A. Manthiram, *Adv. Funct. Mater.* **2023**, *33*, DOI: 10.1002/adfm.202211461.
[34] J. Li, W. Li, Y. You, A. Manthiram, *Adv. Energy Mater.* **2018**, *8*, DOI: 10.1002/aenm.201801957.
[35] M. Yi, R. Sim, A. Manthiram, *Small* **2024**, *20*, e2403429.
[36] Q. Dong, F. Guo, Z. Cheng, Y. Mao, R. Huang, F. Li, H. Dong, Q. Zhang, W. Li, H. Chen, Z. Luo, Y. Shen, X. Wu, L. Chen, *ACS Appl. Energy Mater.* **2020**, *3*, 695.
[37] Q. Xie, W. Li, A. Dolocan, A. Manthiram, *Chem. Mater.* **2019**, *31*, 8886.

Manuscript received: December 21, 2024
Revised manuscript received: February 23, 2025
Accepted manuscript online: February 25, 2025
Version of record online: March 5, 2025